

Title No. 111-S105

Effect of Fiber Material and Loading History on Shear Behavior of Fiber-Reinforced Concrete

by David Carnovale and Frank J. Vecchio

While the benefits of fiber-reinforced concrete (FRC) have been widely investigated, much of the literature focuses on steel FRC subjected to monotonic loads. Data on the structural behavior of macro-synthetic polypropylene FRC or FRC under cyclic loads are scarce.

A pilot investigation on the shear behavior of polypropylene FRC and on the behavior of FRC under reversed cyclic in-plane shear loading was undertaken. Five in-plane shear panel tests were performed. The parameters under study were the fiber material type (steel or polypropylene) and loading protocol. Additionally, a number of compression, direct tension, and flexural tests were performed to determine the material properties of the concretes for comparison. Results show that the material response of 2.0% by volume of polypropylene FRC is nominally similar to that of 1.0% steel FRC.

Keywords: behavior; fiber-reinforced concrete; macro-synthetic; polypropylene; reversed cyclic; shear.

INTRODUCTION

Fiber-reinforced concrete (FRC) is used in many applications, including pavements, airport runways, shotcrete tunnel linings, slabs-on-ground, and when minimum reinforcement is required in precast bridge decks.¹⁻³ In addition, steel fibers have seen limited use in framed slabs and in other flexure-critical structural members.² However, FRC has not been substantially used in more critical structural elements.⁴ This is attributable to the limited research on fiber use in such applications and the lack of development of design codes required for specifying the material.⁵ However, past research on steel fiber-reinforced concrete (SFRC) shear-critical structures have shown that fibers can be used to improve the ductility and better control crack growth in relation to minimum conventional shear reinforcement.^{2,6}

The introduction of fibers alters the brittle tension response of the concrete. Small amounts of fiber addition lead to significant increases in toughness and ductility.⁷⁻⁹ Improvements in crack control can also be achieved.^{6,8} Depending on the fiber aspect ratio, mechanical anchorage, and material strength, steel fiber volume contents of 0.5 to 1.0% have been shown to effectively control cracking and enable behavior similar to that of minimum conventional steel reinforcement.^{6,7} An extensive database of 147 SFRC beams compiled by Parra-Montesinos¹⁰ shows that the addition of 0.75% by volume of steel fibers increases the shear strength of concrete to greater than $0.30\sqrt{f'_c}$ MPa ($0.114\sqrt{f'_c}$ ksi).¹⁰ In addition, fibers prevent localization of excessive diagonal cracking in beam webs, increasing the stiffness and ductility.¹⁰⁻¹² In some cases, the failure mode is changed from shear to flexure.¹² ACI 318¹³ lists SFRC beams in

Section 11.4.6.1 among elements exempt from minimum shear reinforcement.

Polypropylene fibers have not been similarly codified by ACI as more research is required. The benefits to the tension response of concrete are similar⁷ to steel fibers and polypropylene offers corrosion resistance,¹⁴ resistance to alkali attack,¹ low cost,¹⁵ and durability to impact loads.¹⁶ Polypropylene itself is susceptible to fire, yet this is of little concern when embedded in concrete.¹⁴ Micro-synthetic polypropylene fibers (with a diameter less than 0.3 mm [0.012 in.]) have seen limited use in structural applications; they have been more typically used to control shrinkage microcracking.¹⁶ Recently, macro-synthetic polypropylene fibers have been developed with larger diameters and surface treatments that provide mechanical anchorage.¹⁷

As with steel, the addition of polypropylene fibers does not have a significant effect on the cracking strength of concrete.³ In flexure, an increase in peak strength, toughness, and residual strength can be achieved with 0.5% by volume polypropylene fibers.¹⁸ Past experimental programs have shown that steel and polypropylene FRC (PPFRC) can attain similar levels of residual strength and toughness, provided the fiber dosage is scaled in proportion to the material bond strength with concrete (that is, the total volume of polypropylene fibers is increased relative to the volume of steel fibers, in proportion to their bond strength).⁴

In initial post-cracked stages, steel fibers exhibit an improved ability to arrest sudden load decay. The PPFRC exhibits a larger drop in load prior to the arrest of crack growth; a large strain is required before the stress in the fibers will match the stress of the concrete, due to the low modulus of elasticity of polypropylene. This is supported by the findings of many researchers.^{3,19,20} After this initial drop, the PPFRC specimens sustain an increase in residual load-carrying capacity at high crack widths as the low-modulus fiber carries full fiber anchorage without rupture, allowing for energy dissipation.²⁰

It has been shown that synthetic polypropylene fibers can promote improved shear strength and resistance by controlling cracking and allowing tensile stresses to be transmitted across the main diagonal crack.¹⁷ Altoubat et al.¹⁷ performed an extensive study on large-scale PPFRC beams without stirrups using the new-generation macro-synthetic fibers. Both the slender ($a/d \geq 2.5$) and short

ACI Structural Journal, V. 111, No. 5, September-October 2014.

MS No. S-2013-193.R4, doi:10.14359/51686809, was received December 20, 2013, and reviewed under Institute publication policies. Copyright © 2014, American Concrete Institute. All rights reserved, including the making of copies unless permission is obtained from the copyright proprietors. Pertinent discussion including author's closure, if any, will be published ten months from this journal's date if the discussion is received within four months of the paper's print publication.

($a/d \leq 2.5$) beams showed improvements in shear strength. Shear strengths of $0.3\sqrt{f'_c}$ MPa ($0.114\sqrt{f'_c}$ ksi) were achieved using 0.75% PPFRC.¹⁷

Upon first diagonal cracking, the PPFRC beams exhibited a drop in load and an increase in midspan displacement before the crack width opening was arrested and the load-carrying capacity increased.¹⁷ Despite this, the overall deformation capacity was improved and the beams exhibited a gradual and controlled decrease in load after the peak. Altoubat et al.¹⁷ noted that further investigation into shear ductility must be carried out to determine if such fibers may be used in place of minimum stirrups.

In terms of the behavior of FRC structural members under reversed cyclic shear loads, numerous researchers have reported the positive effect on energy dissipation when fiber reinforcement is used in concrete,^{3,21,22} yet specific research on shear-critical cyclically loaded elements is limited.

Research has shown that the addition of steel fibers in beam-column joint regions increases shear strength and reduces crack spacing. This results in increased stiffness and reduced shear deformation. However, in joints with high longitudinal reinforcement ratios, SFRC effectiveness is greatly reduced.²³

Chalioris²² noted that, for shear-critical beams, steel-fiber hysteretic loops showed greater pinching and residual deformation in comparison to plain concrete, suggesting the presence of steel fibers prevents crack closing. Also, reinforcing with stirrups created flexural failure; reinforcing with 0.75% by volume of fibers without stirrups did not change the failure mode. This is contrary to the observed behavior of monotonically loaded shear-critical beams, as noted previously.

For PPFRC under reversed cyclic loads, past studies on elements subjected to reversed cyclic shear loading, while limited, point to improved impact resistance and energy absorption relative to plain concrete.¹⁶

RESEARCH SIGNIFICANCE

The inclusion of fibers in concrete significantly alters the tension response, increasing post-cracked toughness, ductility, and crack control. Such benefits lead to improvements in the shear response of concrete, and may eventually lead to fiber supplanting the use of conventional bars as minimum shear reinforcement in some applications. However, FRC has not been substantially used in critical structural elements. The tests reported herein aim to improve the understanding of the shear behavior of FRC elements containing steel and polypropylene fibers, and to investigate the implications of cyclic loading. Greater understanding is required to improve constitutive modeling of, and confidence in, the material.

EXPERIMENTAL PROGRAM

Susetyo²⁴ performed an extensive research investigation on a series of shear panels with varying types of steel fibers in comparison to low percentages of transverse steel reinforcement. These were tested under pure monotonic in-plane shear loads. Susetyo²⁴ also used compression tests, direct tension tests, and flexural tests to study SFRC behavior

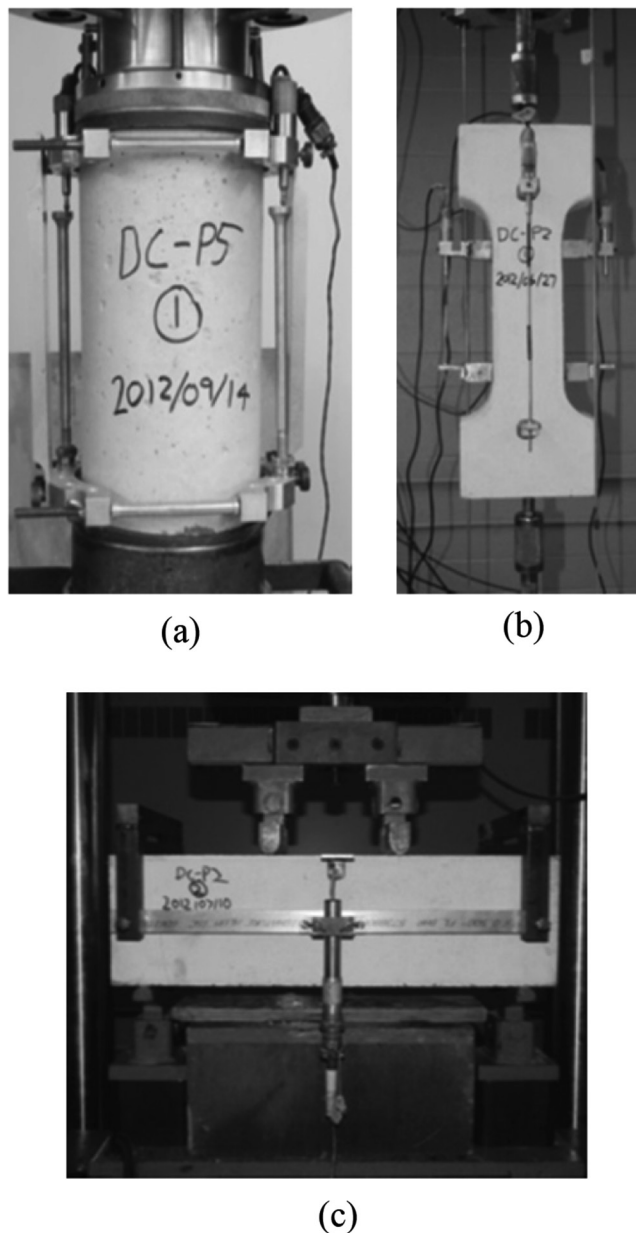


Fig. 1—Material test specimens.

(depicted in Fig. 1). Building upon this program, the study described in this paper investigated the influence of fiber type (steel versus polypropylene) and loading protocol (monotonic versus reversed cyclic) on FRC compressive, tensile, flexural, and shear behavior. Some of the Susetyo²⁴ test sets were used for comparison. Thus, the test matrix shown in Table 1²⁵ was formulated. It is worth noting that two preliminary tension test sets were carried out to investigate the effect of fiber-volume fraction on PPFRC response.²⁵

Materials

The mixture designs used are summarized in Table 2; the target characteristic compressive strength was 50 MPa (7.25 ksi). The concrete was batched and mixed using the facilities at the University of Toronto. Once the specimens were cast and finished, they were covered with layers of wet burlap and plastic and left to cure for 7 days. After this, the

Table 1—Test matrix

Series name	f'_c , MPa (ksi)	Fiber type	V_f , %	Loading protocol
Tests performed by Carnovale ²⁵				
DC-DB1	50 (7.25)	MAC matrix	2.0	—
DC-DB2	50 (7.25)	MAC matrix	3.0	—
DC-P1	50 (7.25)	—	—	Reversed cyclic
DC-P2	50 (7.25)	RC80/30BP	1.0	Monotonic
DC-P3	50 (7.25)	MAC matrix	2.0	Monotonic
DC-P4	50 (7.25)	RC80/30BP	1.0	Reversed cyclic
DC-P5	50 (7.25)	MAC matrix	2.0	Reversed cyclic
Tests performed by Susetyo ²⁴				
C1C	50 (7.25)	—	—	Monotonic
C1F1V1	50 (7.25)	RC80/50BN	0.5	Monotonic
C1F1V2	50 (7.25)	RC80/50BN	1.0	Monotonic
C1F1V3	50 (7.25)	RC80/50BN	1.5	Monotonic

Table 2—Concrete mixture design

Material	Unit	OPC	SFRC ($V_f = 1.0\%$)	PPFRC ($V_f = 2.0\%$)
Type 10 cement	kg (lb)	375 (827)	500 (1102)	500 (1102)
Water	kg (lb)	139 (306)	200 (441)	200 (441)
Sand	kg (lb)	847 (1867)	1114 (2456)	1114 (2456)
10 mm (0.4 in.) limestone coarse aggregate	kg (lb)	1080 (2381)	792 (1746)	792 (1746)
High-range water-reducer	mL (oz)	3300 (111.6)	3670 (124.1)	4000 (135.3)
Steel fibers	kg (lb)	—	78.5 (173.1)	—
Polypropylene fibers	kg (lb)	—	—	18.2 (40.1)
Slump	mm (in.)	70 (2-3/4)	170 (6-11/16)	110 (4-5/16)

specimens were demolded and left to age under ambient conditions.

Conventional steel reinforcement was used only in the shear panel specimens. The mechanical properties of the steel are shown in Table 3. Three fiber types were used in the experimental tests discussed herein.

The fiber properties are summarized in Table 4. It is worth noting herein that the modulus of elasticity of the polypropylene fiber is 1/20 that of the steel fibers. Thus, if the orientation of the fibers across the crack is the same, then a much higher strain (and thus, crack width) is required to transmit similar stresses across the crack. At low strains, the steel

Table 3—Reinforcement properties

Bar type	d_b , mm (in.)	A_b , mm ² (in. ²)	E_s , GPa (ksi)	f_y , MPa (ksi)	ϵ_y , $\times 10^{-3}$	f_u , MPa (ksi)	ϵ_w , $\times 10^{-3}$
D4 (DC series)	5.72 (7/32)	25.81 (0.040)	184 (26,700)	484.3 (70.2)	2.67	624.4 (90.6)	22.7
D8 (DC series)	8.10 (3/8)	51.61 (0.080)	193 (27,900)	466.4 (67.6)	2.43	605.4 (87.8)	37.1
D4 (C1 series)	5.72 (7/32)	25.81 (0.040)	187 (27,000)	446.9 (64.8)	2.41	548.9 (79.6)	57.6
D8 (C1 series)	8.10 (3/8)	51.61 (0.080)	225 (32,500)	555.2 (80.5)	2.58	647.2 (93.9)	45.4

Table 4—Fiber properties

Fiber	l_f , mm (in.)	d_f , mm (in.)	AR_f	f_{uf} , MPa (ksi)	E_f , MPa (ksi)
RC80/30BP	30 (1-3/16)	0.38 (0.015)	79	2300 (333.6)	200,000 (29,000)
RC80/50BN	50 (2)	0.62 (0.024)	81	1050 (152.3)	200,000 (29,000)
MAC matrix	54 (2-1/8)	0.81 (0.032)	67	520 (75.4)	10,000 (1450)

fibers are able to carry much higher stresses. This became evident throughout the experimental program.²⁵

Specimens

Cylinder compression tests—Cylinder tests were performed to evaluate the compressive behavior of the concrete, including the peak strength, strain at peak stress, and elastic modulus in compression (secant modulus to 40% of the peak stress). The 152 mm (6 in.) diameter cylinders were tested at 28 days in an MTS stiff frame testing machine at a loading rate of 0.005 mm/s (0.0002 in./s). Two linear variable differential transducers (LVDTs) with a gauge length of 250 mm (10 in.) were used to measure displacements.

Uniaxial direct tension tests—It was important to investigate the contribution of the fibers in direct tension to observe the improvements in post-cracked behavior, ductility, and toughness. Thus, 70 mm (2.75 in.) thick direct tension “dogbone” specimens were used with inner neck dimensions of 100 x 300 mm (4 x 12 in.) and overall dimensions of 200 x 500 mm (8 x 20 in.); Fig. 1 depicts the specimen shape. Because the cracking location in concrete is highly variable, two 300 mm (12 in.) LVDTs were used (although these LVDTs encompassed the change in cross section) to ensure the crack was captured. Two short (150 mm [6 in.]) LVDTs were also provided on the narrowed portion of the specimen. Further details can be found in the Appendix.*

*The Appendix is available at www.concrete.org/publications in PDF format, appended to the online version of the published paper. It is also available in hard copy from ACI headquarters for a fee equal to the cost of reproduction plus handling at the time of the request.

The specimens were tested in a 55 kip (245 kN) MTS universal testing machine under external displacement control at an initial loading rate of 0.001 mm/s (0.00004 in./s). When the peak residual load after cracking was reached, the loading rate was gradually increased to a maximum of 0.01 mm/s (0.0004 in./s). The tests concluded when load capacity decayed to approximately 20% of the maximum residual load.

Flexural tests—Flexural tests were performed on un-notched specimens and in accordance with ASTM C1609.²⁶ The beam specimens had dimensions of 152 x 152 x 533 mm (6 x 6 x 21 in.). The clear span between supports was 457 mm (18 in.) and the locations of the loading points were 152 mm (6 in.) from each support (that is, quarter-point loading). Two LVDTs were used to measure the midspan displacement on each vertical face of the beam. A rectangular mounting rig was used to position these LVDTs at the beam midheight.

The specimens were tested in a 1000 kN (225 kip) MTS four-post test machine at a rate of 0.006 mm/s (0.00024 in./s). The typical test continued at this rate until a peak residual load was obtained, at which point the loading rate was increased gradually up to a maximum of 0.02 mm/s (0.0008 in./s). The test continued until a midspan deflection of $L/60$ was achieved.

Panel tests—The goal of the panel tests was to investigate and compare the structural response of SFRC and PPFRC under in-plane pure shear and to also compare the results against conventional reinforced concrete members. The panel tests were performed using the Panel Element Test Facility at the University of Toronto (Fig. 2 and Fig. A1), designed to subject square panel elements (890 x 890 x 70 mm [35 x 35 x 2.75 in.]) to uniform in-plane stress conditions. The machine consists of 37 hydraulic cylinders and three rigid links. Two of the three rigid links connect at one steel shear key, creating a pin connection, while the other rigid link acts as a vertical roller. To restrain the specimen from out-of-plane movements, tension links are used to connect the keys to a back frame. Each hydraulic jack has a capacity of 218.2 kN (49.1 kip) in compression and 95.6 kN (21.5 kip) in tension.

The panel reinforcement layout used is depicted in Fig. A2. The plain concrete panels were reinforced with 40 D8 deformed wires in the longitudinal direction ($\rho_x = 3.31\%$) and 10 D4 deformed wires in the transverse direction ($\rho_y = 0.42\%$) to represent relatively low amounts of transverse reinforcement. It is worth noting that at least two D4 bars were required for each shear key to provide adequate anchorage and transmit the forces necessary for failure of the panel specimen. The FRC panels contained 40 D8 deformed wires in the longitudinal direction ($\rho_x = 3.31\%$; $\rho_y = 0$), as the desire was to compare the behavior using low percentages of transverse conventional steel reinforcement to that of SFRC and PPFRC. Forty 5/16 in. threaded rods were provided in the transverse direction to anchor the shear keys (Fig. A2).

To measure strains, a total of 12 LVDTs were used. Each face of the panel was instrumented with two LVDTs

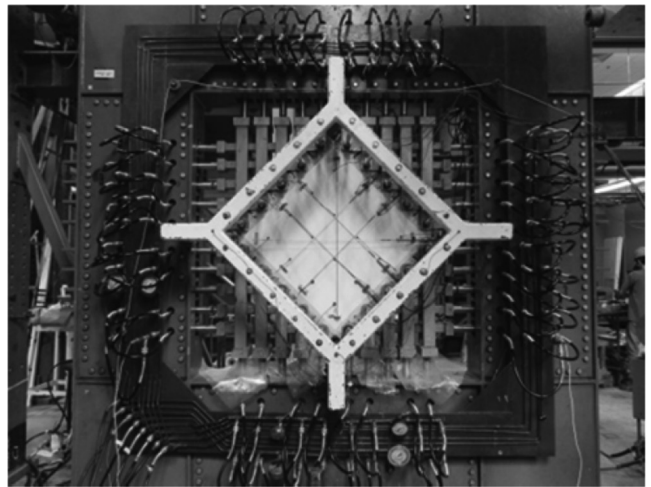


Fig. 2—Panel specimen in Panel Element Test Facility.

placed in the x-direction, two in the y-direction (740 mm [29 in.] long), one in the 45-degree direction, and one in the 135-degree direction (1000 mm [40 in.] long). Loads were applied using a hydraulic load maintainer under a force control mode. During each loading phase, the load maintainer was manually operated until the target shear stress was attained. Once achieved, a “load stage” was defined where a load was held constant while strain readings were taken and cracks were marked and measured. For the monotonic tests, loading continued in one direction until failure. With the reversed cyclic tests, the load was reduced to zero and the panel was reloaded in the opposite shear direction. Double cycles were taken at each target stress level.

EXPERIMENTAL RESULTS AND DISCUSSION

Influence of fiber type

Compression response—As shown in Table 5, the plain concrete attained the highest peak compressive strength, followed by concrete with short steel fibers. Fiber addition negatively affected concrete compaction, leading to a decrease in concrete strength; however, other aspects of the compressive stress-strain response were not significantly affected by the addition of the fibers. No systematic differences between the modulus of elasticity at low loads were observed between concretes with different fiber types or volumes (refer to Table A1).

The strain at the peak stress and ductility were increased through the use of FRC (as shown in Fig. 3(a)). The load-carrying capacity of plain concrete in compression dropped suddenly after the peak, whereas the stress decay in the FRC was more gradual. This led to improved ductility and toughness as the FRC reached strains of at least 300% of ϵ'_c before failure. Immediately after reaching the peak, the load for PPFRC specimens dropped in a fashion similar to that of C1F1V1, which contained 0.5% by volume steel fibers. Yet, as the strain increased further, the PPFRC specimens exhibited an improved residual strength capacity, close to that of C1F1V2 (1.0% steel fibers). The overall compressive response for PPFRC was similar to that of SFRC containing end-hooked steel fibers of similar length. Supplementary

Table 5—Panel element test results

ID	f'_{cs} MPa (ksi)	v_{crs} MPa (ksi)	γ_{crs} $\times 10^{-3}$	v_{us} MPa (ksi)	γ_{us} $\times 10^{-3}$	w_m mm (in.)	s_m mm (in.)	$f_{c1,crs}$ MPa (ksi)	$f_{c1,max}$ MPa (ksi)	$f_{c1,us}$ MPa (ksi)	$f_{c2,us}$ MPa (ksi)	f_{ss} MPa (ksi)	f_{sy} MPa (ksi)	Failure mode
DC-P1	71.7 (10.40)	1.43 (0.21)	0.116	5.79 (0.84)	7.98	0.57 (0.022)	55.6 (2.19)	1.43 (0.21)	2.82 (0.41)	0.65 (0.09)	-11.63 (-1.69)	267 (38.7)	611 (88.6)	y-reinforcement rupture
DC-P2	62.1 (9.01)	2.60 (0.38)	0.136	5.97 (0.87)	5.94	0.21 (0.008)	43.0 (1.69)	2.49 (0.36)	3.37 (0.49)	2.95 (0.43)	-12.05 (-1.75)	275 (39.9)	—	Interlock failure
DC-P3	50.9 (7.38)	2.20 (0.32)	0.153	3.87 (0.56)	7.96	0.57 (0.022)	72.0 (2.83)	2.13 (0.31)	2.42 (0.35)	1.73 (0.25)	-8.69 (-1.26)	210 (30.5)	—	Interlock failure
DC-P4	64.0 (9.28)	2.60 (0.38)	0.136	4.47 (0.65)	2.87	0.22 (0.009)	71.0 (2.80)	2.60 (0.38)	3.54 (0.51)	2.59 (0.38)	-7.66 (-1.11)	153 (22.2)	—	Interlock failure
DC-P5	54.3 (7.88)	2.23 (0.32)	0.104	3.43 (0.50)	5.15	0.59 (0.023)	59.0 (2.32)	2.12 (0.31)	2.56 (0.37)	1.27 (0.18)	-3.83 (-0.56)	204 (29.6)	—	Interlock failure
C1C	65.7 (9.53)	2.01 (0.29)	0.086	5.77 (0.84)	6.01	0.55 (0.022)	57.2 (2.25)	2.05 (0.30)	2.87 (0.42)	1.43 (0.21)	-11.70 (-1.70)	250 (36.3)	501 (72.7)	y-reinforcement yielding
C1F1V1	51.4 (7.45)	2.09 (0.30)	0.197	3.53 (0.51)	2.77	0.55 (0.022)	114.4 (4.50)	2.21 (0.32)	2.83 (0.41)	1.85 (0.27)	-6.73 (-0.98)	148 (21.5)	—	Interlock failure
C1F1V2	53.4 (7.75)	2.65 (0.384)	0.139	5.17 (0.75)	5.27	0.45 (0.018)	54.7 (2.15)	2.59 (0.38)	3.04 (0.44)	2.82 (0.41)	-9.46 (-1.37)	201 (29.2)	—	Interlock failure
C1F1V3	49.7 (7.21)	1.83 (0.27)	0.055	5.37 (0.78)	5.10	0.45 (0.018)	57.2 (2.25)	1.85 (0.27)	3.13 (0.45)	2.97 (0.43)	-9.70 (-1.41)	204 (29.6)	—	Interlock failure

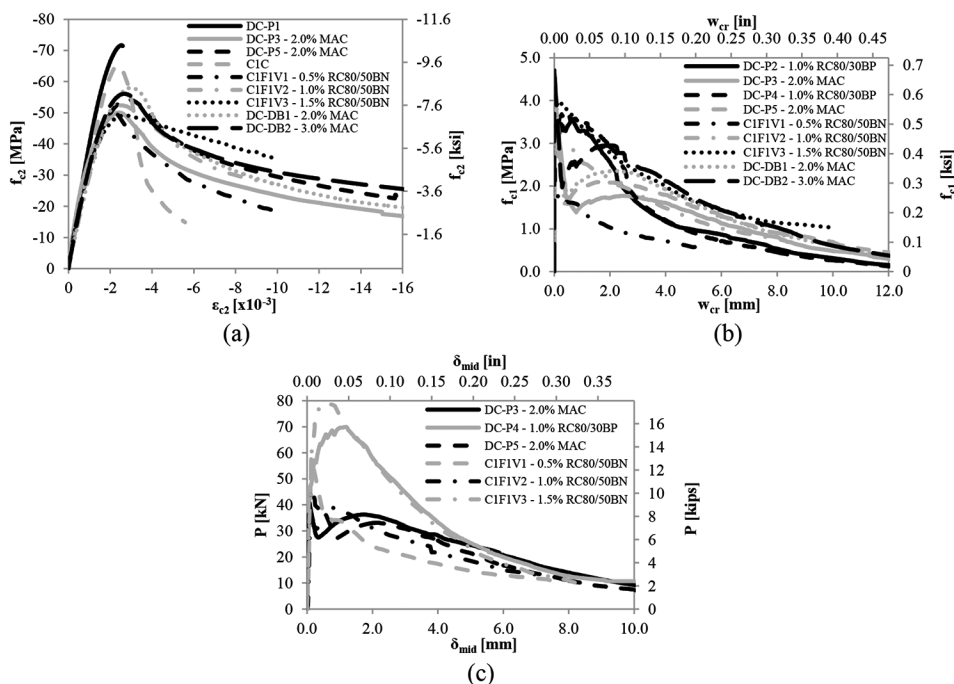


Fig. 3—Influence of fiber material on: (a) compression; (b) direct tension; and (c) flexural responses.

information for the cylinder compression tests can be found in Table A1 of the Appendix.

Direct tension response—The effects of fiber addition on the properties of the concrete prior to cracking were negligible. After cracking, the plain concrete exhibited a brittle failure, whereas the FRC specimens exhibited ductility.

The influence of the fiber type is presented graphically in Fig. 3(b). The crack width at fiber engagement for the steel fibers was consistent, but the magnitude of the initial drop

in load to this point of engagement was inversely proportional to the fiber-volume content. At large crack widths, the SFRC with shorter fibers began to rapidly lose load-carrying capacity and the residual stress dropped below that of the longer steel fibers and polypropylene fibers.

The response was different for the PPFRC specimens. The initial stress decay after cracking was larger, as a large crack width (and strain) was required before the polypropylene fibers engaged.¹⁹ The maximum residual tensile

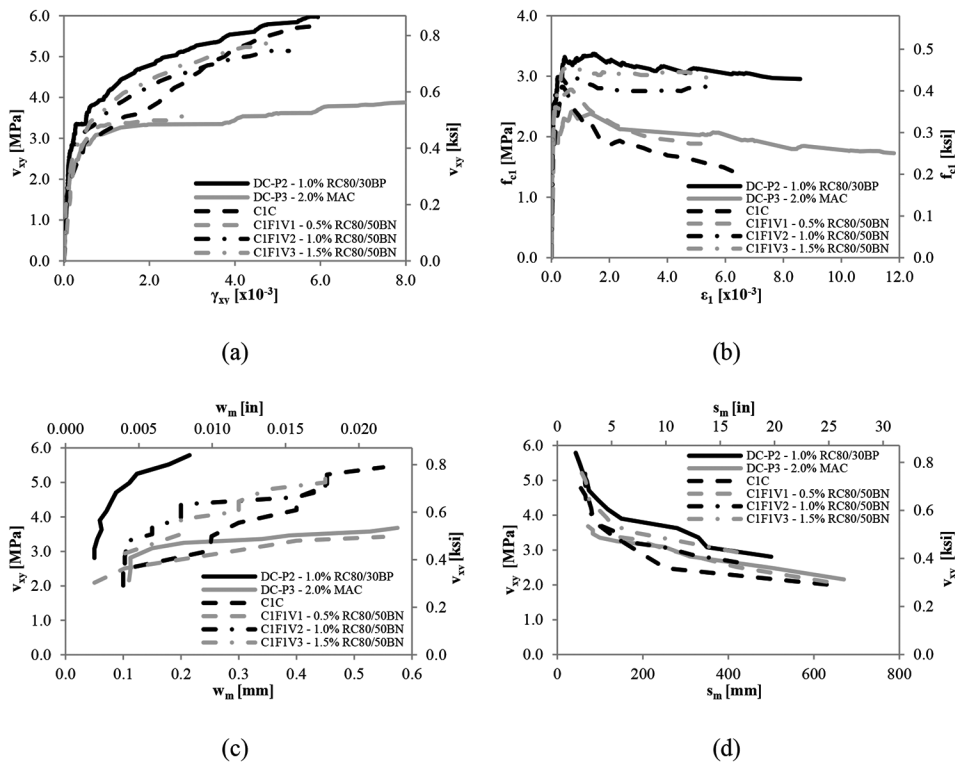


Fig. 4—Influence of fiber material on shear response.

stress was as much as 150% of the stress at engagement but occurred at large crack widths. At crack widths above 2.5 mm (0.1 in.), the steel fibers began to lose bond strength due to the straightening of the end hook or local concrete deterioration⁵; the PPFRC did not exhibit this response. At 3 mm (0.12 in.), the polypropylene specimens consistently exhibited high residual load-carrying capacities. However, in service, such large crack widths are not desirable; thus, within practical limits, polypropylene fibers are in need of improvement in terms of bond strength and fiber stiffness. It can be seen that the stress at fiber engagement for 2.0% PPFRC was similar to 0.5% SFRC, and the residual load-carrying capacity for 2.0% PPFRC was similar to 1.0% SFRC at large crack widths (at the cost of reduced load-carrying capacity at small crack widths). Further results can be found in Table A2.

Flexural response—The load-deflection responses are depicted in Fig. 3(c). The observations that can be made in flexural tension are similar to those for direct tension. The short steel fibers were most effective in residual load-carrying capacity. Concretes with as little as 1.0% of the short fibers experienced elevated amounts of deflection hardening and attained the greatest peak load. Just as with direct tension, the longer fibers exhibited more ductility at large crack widths.

From the PPFRC responses, it was clear that at low crack widths, the polypropylene fibers did not become sufficiently engaged. However, at high midspan displacements, these fibers proved effective in sustaining a gradual release of load. At a midspan displacement of over 4 mm (0.16 in.), specimens containing PPFRC showed the greatest residual flexural load-carrying capacity. The values of toughness and

equivalent flexural strength ratio (to a deflection of $L/150$) for DC-P5 with 2.0% PPFRC (96.3 J [71.0 ft-lbf] and 81.3%, respectively) were similar to those of C1F1V2 with 1.0% SFRC (103 J [76.0 ft-lbf] and 74.2%, respectively). As with direct tension, the polypropylene fibers provided residual load-carrying capacity, toughness, and ductility similar to that of 1.0% steel fibers with the same length, with an initial reduced load-carrying capacity. Further test results can be found in Table A3.

Shear panel response—Table 5 presents pertinent results from the panel tests. Also, Fig. 4 depicts the responses of six of the panels tested under monotonic shear loading. Included in this figure are graphs of shear stress versus shear strain, principal tensile stress versus principal tensile strain, shear stress versus mean crack width, and shear stress versus mean crack spacing.

Shear resistance and ductility—The SFRC specimens, with the exception of C1F1V1, achieved similar shear strengths and ductilities to those of the Control Panel C1C. The addition of 1.0% by volume of end-hooked steel fibers is a viable option for replacing 0.42% of conventional steel. DC-P2, for example, achieved a 3.5% increase in shear strength with only a 1.2% reduction in ductility when compared to reinforced concrete. The light volume fraction of steel fibers in C1F1V1 (0.5%) was insufficient in developing adequate strength and ductility.

The PPFRC specimen, DC-P3, was similarly unable to achieve an equivalent shear strength (3.87 MPa [0.56 ksi], a 32.9% reduction compared to C1C), yet the shear strain at ultimate was increased by 32.4%. This panel achieved a failure strain significantly greater than any of the others tested, achieving an ultimate shear strain that was 132%

that of C1C, and 151% that of C1F1V2 (even though the length of the polypropylene fibers and the steel fibers used in C1F1V2 were similar). These fibers showed an ability to bridge large cracks without significant fiber pullout or rupture, improving toughness and ductility, evidenced by the large shear strains at failure shown in Fig. 4(a) and the large crack widths in Fig. 4(c).²⁰ The strength achieved by DC-P3 was 11% greater than that of C1F1V1, meaning that the shear strength capacity of this specimen was similar to that of 0.5% SFRC. These improvements in ductility seen in Fig. 4(a) are not sufficient to warrant the full replacement of conventional steel with polypropylene fibers due to the loss of shear strength relative to the Control Panel C1C.

Principal tensile responses—The behaviors observed with respect to shear strength and ductility were also apparent in the principal tensile behavior. After cracking, all of the SFRC specimens exhibited similar maximum tensile strengths to that of the control specimen. The PPFRC specimen reached a maximum tensile stress of 16% less than C1C and 23% less than the 1.5% SFRC panel. This supports the finding of the relatively low engagement of these fibers at low crack widths as a result of the low fiber stiffness and lack of mechanical anchorage.¹⁹ However, the residual load-carrying capacity of the PPFRC specimen showed improvement over that of plain reinforced concrete and was similar to that of C1F1V1. Tension ductility, on the other hand, was improved through the use of polypropylene fibers. The ultimate tensile strain achieved by each of the panels containing long end-hooked steel fibers was similar, suggesting that the cracking sustained at a principal tensile strain of approximately 6.0×10^{-3} was the maximum attainable for these types of fibers. However, the polypropylene FRC withstood at least 1.75 MPa (0.254 ksi) of residual tensile stress to a much higher ultimate tensile strain of 11.8×10^{-3} . The ultimate tensile strain of PPFRC was 188% that of C1C and 211% that of C1F1V2, but the ultimate tensile stress was reduced by 39% relative to that of C1F1V2.

Crack control characteristics—At nearly all levels of applied stress, the crack widths in the DC-P3 panel were similar to those of Panel C1F1V1 and greater than those of the high-volume SFRC specimens. This was also true of average crack spacings, as the PPFRC panel exhibited larger crack spacing (meaning fewer individual cracks) at most levels of applied stress. This observation suggested that these fibers experienced difficulty in transmitting enough stress across a crack to form subsequent cracks at the fiber-volume fraction used.³ However, the fact that these large cracks were sustained without failure suggests that PPFRC can sustain significant damage, as the fibers remain anchored to the concrete up to large crack widths.²⁰ DC-P2, with short steel fibers, exhibited the smallest crack widths and tightest crack spacings.

Failure mode—The failure crack patterns for each of the panels are shown in Fig. A3. All of the FRC panels failed by shear slip after fiber pullout across the main cracks. The plain concrete specimens experienced rupture of the y-direction reinforcement and shear slip. The failure plane orientation became more aligned with the x-direction steel as a result of both the load cycling and the use of polypropylene fibers.

Influence of loading protocol

Plain reinforced concrete—The cyclically loaded plain concrete specimen, DC-P1, did not experience any stress degradation and, in fact, achieved a 33% increase in shear ductility compared to the monotonically loaded Panel C1C (Fig. 5). Conversely, the residual principal tensile stress capacity was negatively affected as expected. This can be explained by the higher strength of the transverse direction steel reinforcement in the cyclic test (DC-P1) relative to the monotonic test (C1C) (as seen in Table 5). A higher shear stress was attained before failure as the steel shear reinforcement carried more load. DC-P1 exhibited greater crack control (smaller average crack widths at a given stress), yet the overall behavior was similar to the monotonic test.

SFRC—Fig. 6 shows that the shear resistance and ductility of the SFRC specimen was greatly affected by the loading protocol. The maximum shear stress attained by DC-P4 was reduced by 25% compared to DC-P2; the ultimate shear strain was reduced by 52% as a result of the cycling of load. This is consistent with the result of past experimental findings of SFRC beams tested under reversed cyclic shear loads.²²

The maximum principal tensile stress achieved by DC-P4 was similar to that of DC-P2; however, as load cycling progressed, the residual tensile load-carrying capacity began to degrade. The average crack spacing for DC-P4 at a given shear stress was larger than that of DC-P2, indicating that the ability of the fibers to transmit enough stress across existing cracks and generate further cracking had diminished. The tensile strain continued to increase to a maximum of 6.75×10^{-3} , a 21% reduction when compared to the monotonic test. The average crack widths at failure were identical to those of the monotonic test, meaning that load cycling led to breakdown of fiber ability to control the crack widths and promote adequate aggregate interlock. In addition, the eventual failure plane of DC-P4 was steeply inclined, suggesting an increased rotation of the principal tensile direction as a result of cyclic loading. Thus, the reversed cyclic loading protocol was substantially detrimental to the behavior of the SFRC specimens containing these short fibers.

Polypropylene FRC—The responses of DC-P3 and DC-P5 are presented in Fig. 7. Again, the shear response was detrimentally affected by the reversed cyclic loading protocol. The maximum shear stress attained was reduced by 11% and the ultimate shear strain was reduced by 35%. However, when compared to the degradation experienced by the SFRC panel, the degree of degradation was not as severe. Average crack spacing and average crack widths for PPFRC were similar throughout the duration of the cyclic test, meaning that the ability of these fibers to transmit tensile stresses across the cracks and generate further cracking was not as detrimentally affected as in SFRC by the crack slip and lack of crack closing caused by the reversed cyclic loading protocol. At failure, the principal tensile strain attained was 10.9×10^{-3} , which represented a relatively small reduction of 7.4% as compared to the monotonic test. The crack spacing and crack width at failure, and the failure plane, were nearly identical between the monotonic and reversed cyclic test. Except for the final cycle, the maximum tensile stress and

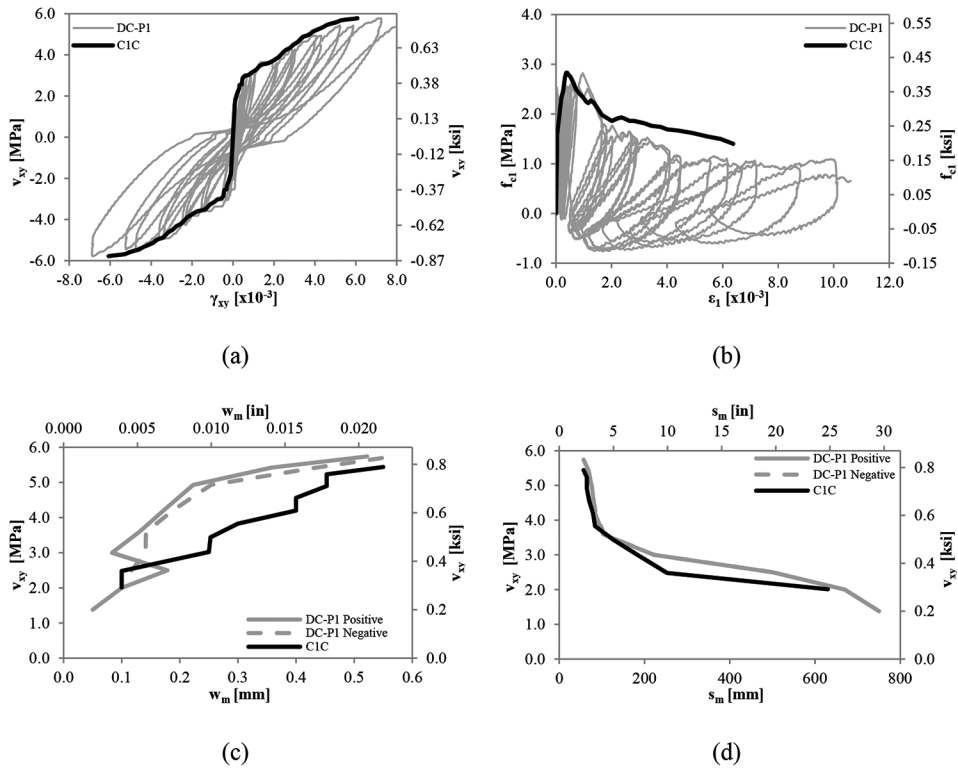


Fig. 5—Influence of loading protocol on reinforced concrete shear response.

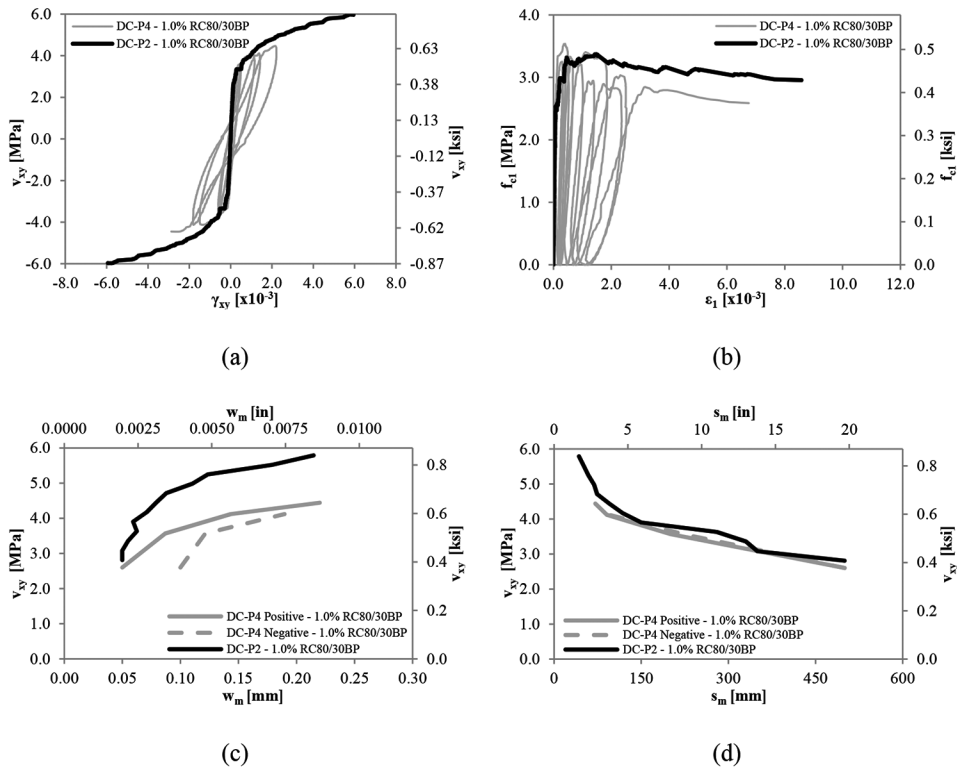


Fig. 6—Influence of loading protocol on SFRC shear response.

strain attained for most of the cycles matched closely with that of the monotonically loaded DC-P3.

Comparison—The load-carrying capacity and crack-bridging tendencies of short, stiff, end-hooked steel fibers were reduced when a cyclic loading regime was imposed. After completion of the tests, the steel fibers subjected to

cyclic loading exhibited a wavy shape, evidence of plastic fiber deformation due to repetitive stretching, and buckling of the fibers.²³ Conversely, the crack control characteristics and principal tensile stress-strain response of the PPFRC specimen showed that long, flexible polypropylene fibers did not suffer the same degree of degradation. The low stiff-

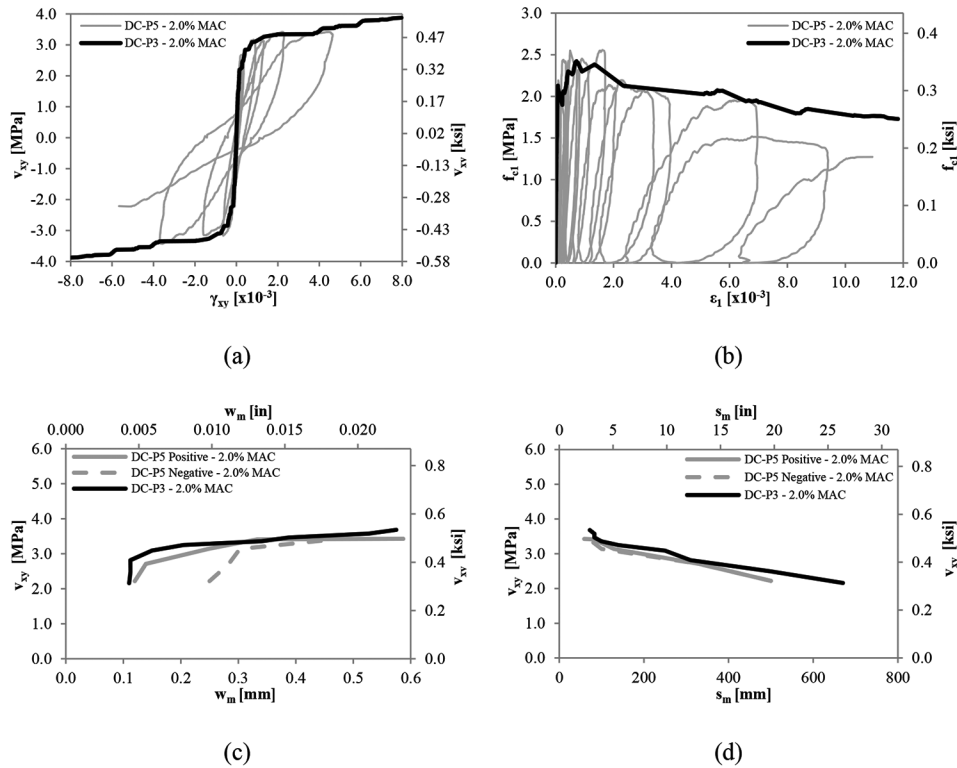


Fig. 7—Influence of loading protocol on PPFRC shear response.

ness of the fibers allowed for flexibility during crack slip, preventing the breakdown of fiber-concrete bond. The total energy absorption was better when PPFRC fibers were used. However, full stirrup replacement using fibers for shear-critical structures subjected to reversed cyclic loads is not yet possible.²³

SUMMARY AND CONCLUSIONS

The influence of fiber material type (steel versus polypropylene) was investigated through a series of compression, direct tension, flexural, and shear tests. In addition, the effect of loading protocol (monotonic versus reversed cyclic) on the shear response of SFRC and PPFRC was studied. The intent of the experimental investigation was to improve the understanding of FRC behavior such that constitutive models and designer confidence in the material could be developed. The results of this pilot investigation suggest the following conclusions:

1. The characteristic benefits of steel fiber addition (in terms of post-cracking residual strength, tensile ductility, and control of crack widths) can also be achieved with polypropylene fibers but with a reduced initial load-carrying capacity.
2. Short steel fibers provide the greatest structural improvements in terms of strength. These fibers, as well as high percentages of long steel fibers, may be used in place of low percentages of conventional transverse steel reinforcement for shear resistance, as confirmed by beam tests compiled by Parra-Montesinos.¹⁰
3. Replacement of minimum transverse steel with polypropylene fibers is not advisable at present; bond technologies and fiber stiffness must be improved before sufficient PPFRC shear strength can be assured.

4. First-cracking of PPFRC in the fiber-volume fractions investigated was accompanied by a sharp drop in load and the development of large crack widths. However, improvements in ductility were achieved, as polypropylene fibers can transmit relatively high amounts of tensile stress across large crack widths.

5. For fibers of similar length, concrete with 2.0% by volume of polypropylene fibers exhibits an overall structural response roughly similar to that of 1.0% steel fibers, albeit with a reduction in load-carrying capacity at small crack widths.

6. The degradation of SFRC response due to reversed cyclic loading is significant, and crack bridging abilities are negatively affected.

7. The degradation of PPFRC response due to reversed cyclic loading is not as sizeable, suggesting that polypropylene fibers may be better for such loading conditions.

8. Complete replacement of minimum transverse conventional steel reinforcement with fibers, for cyclic load applications, is not yet advisable in situations where shear strength is a primary concern. Some fiber replacement remains possible due to the energy dissipation characteristics of fiber reinforcement. This is an attractive possibility for congested beam-column joint regions.

AUTHOR BIOS

David Carnovale is a Project Associate at Halsall Associates in Toronto, ON, Canada. He received his bachelor's and master's degrees in civil engineering from the University of Toronto, Toronto, ON, Canada. His research interests include researching and specifying innovative structural materials.

Frank J. Vecchio, FACI, is a Professor in the Department of Civil Engineering at the University of Toronto. He is a member of Joint ACI-ASCE Committees 441, Reinforced Concrete Columns, and 447, Finite Element Analysis of Reinforced Concrete Structures. His research interests include nonlinear analysis and design of reinforced concrete structures, constitutive

ACKNOWLEDGMENTS

The authors wish to express their gratitude and sincere appreciation to E. Attigbe and BASF for supporting this research work.

NOTATION

A_b	=	steel reinforcing bar area
A_f	=	fiber cross-sectional area
AR_f	=	aspect ratio of fiber
a/d	=	shear span-depth ratio
d_b	=	reinforcing bar diameter
d_f	=	fiber diameter
E_f	=	fiber modulus of elasticity
E_s	=	reinforcing bar modulus of elasticity
f_c'	=	28-day compressive strength of concrete
f_{c1}	=	principal tensile stress of concrete
$f_{c1,cr}$	=	principal tensile stress of concrete at cracking
$f_{c1,max}$	=	maximum principal tensile stress of concrete
$f_{c1,u}$	=	principal tensile stress of concrete at ultimate
f_{c2}	=	principal compressive stress of concrete
$f_{c2,u}$	=	principal compressive stress of concrete at ultimate
f_{sx}	=	x-direction reinforcement stress
f_{sy}	=	y-direction reinforcement stress
f_u	=	ultimate strength
f_{uf}	=	ultimate tensile strength of fiber
f_y	=	yield strength
l_f	=	fiber length
P	=	applied load
s_m	=	mean crack spacing
V_f	=	fiber-volume fraction
v_{cr}	=	cracking shear stress
v_u	=	ultimate shear stress
v_{xy}	=	shear stress
w_{cr}	=	crack width
w_m	=	mean crack width
δ_{mid}	=	midspan displacement
ϵ_1	=	principal tensile strain
ϵ_2	=	principal compressive strain
ϵ_c'	=	strain at peak compressive stress
ϵ_u	=	ultimate strain
ϵ_y	=	yield strain
γ_{cr}	=	cracking shear strain
γ_u	=	ultimate shear strain
γ_{sy}	=	shear strain
ρ_x	=	reinforcement ratio in x-direction
ρ_y	=	reinforcement ratio in y-direction

REFERENCES

1. Wang, Y.; Backer, S.; and Li, V. C., "An Experimental Study of Synthetic Fibre Reinforced Cementitious Composites," *Journal of Materials Science*, V. 22, No. 12, 1987, pp. 4281-4291.
2. Meda, A.; Minelli, F.; Plizzari, G. A.; and Riva, P., "Shear Behaviour of Steel Fibre Reinforced Concrete Beams," *Materials and Structures*, V. 38, 2005, pp. 343-351.
3. Bentur, A., *Fibre Reinforced Cementitious Composites*, second edition, S. Mindess, ed., Taylor & Francis, New York, 2007, 449 pp.
4. Richardson, A. E., and Landless, S., "Synthetic Fibres and Steel Fibres in Concrete with Regard to Bond Strength and Toughness." *Northumbria Working Paper Series: Interdisciplinary Studies in the Built and Virtual Environment*, V. 2, No. 2, 2009, pp. 128-140.

5. Lee, S. C.; Cho, J. Y.; and Vecchio, F. J., "Simplified Diverse Embedment Model for SFRC Elements in Tension," *ACI Materials Journal*, V. 110, No. 4, July-Aug. 2013, pp. 403-412.
6. Susetyo, J.; Gauvreau, P.; and Vecchio, F. J., "Effectiveness of Steel Fiber as Minimum Shear Reinforcement," *ACI Structural Journal*, V. 108, No. 4, July-Aug. 2011, pp. 488-496.
7. Shah, S. P., and Rangan, B. V., "Fiber Reinforced Concrete Properties," *ACI Journal Proceedings*, V. 68, No. 2, Feb. 1971, pp. 126-137.
8. Batson, G., "Steel Fiber Reinforced Concrete," *Materials Science and Engineering*, V. 25, 1976, pp. 53-58.
9. Thomas, J., and Ramaswamy, A., "Mechanical Properties of Steel Fiber-Reinforced Concrete," *Journal of Materials in Civil Engineering*, ASCE, V. 19, No. 5, 2007, pp. 385-392.
10. Parra-Montesinos, G. J., "Shear Strength of Beams with Deformed Steel Fibers," *Concrete International*, V. 28, No. 11, Nov. 2006, pp. 57-66.
11. Choi, K. K.; Park, H. G.; and Wight, J. K., "Shear Strength of Steel Fiber-Reinforced Concrete Beams without Web Reinforcement," *ACI Structural Journal*, V. 104, No. 1, Jan.-Feb. 2007, pp. 12-21.
12. Aoude, H.; Belghiti, M.; William, D. C.; and Mitchell, D., "Response of Steel Fiber-Reinforced Concrete Beams with and without Stirrups," *ACI Structural Journal*, V. 109, No. 3, May-June 2012, pp. 359-367.
13. ACI Committee 318, "Building Code Requirements for Structural Concrete (ACI 318-08) and Commentary," American Concrete Institute, Farmington Hills, MI, 2008, 473 pp.
14. Zheng, Z., and Feldman, D., "Synthetic Fibre-Reinforced Concrete," *Progress in Polymer Science*, V. 20, No. 2, 1995, pp. 185-210.
15. Richardson, A. E., "Bond Characteristics of Structural Polypropylene Fibres in Concrete with Regard to Post-Crack Strength and Durable Design," *Structural Survey*, V. 23, No. 3, 2005, pp. 210-230.
16. Soroushian, P.; Khan, A.; and Hsu, J., "Mechanical Properties of Concrete Materials Reinforced with Polypropylene or Polyethylene Fibers," *ACI Materials Journal*, V. 89, No. 6, Nov.-Dec. 1992, pp. 535-540.
17. Altoubat, S.; Yazdanbakhsh, A.; and Rieder, K. A., "Shear Behavior of Macro-Synthetic Fiber-Reinforced Concrete Beams without Stirrups," *ACI Materials Journal*, V. 106, No. 4, July-Aug. 2009, pp. 381-389.
18. Roesler, J. R.; Altoubat, S. A.; Lange, D. A.; Rieder, K.; and Ulreich, G. R., "Effect of Synthetic Fibers on Structural Behavior of Concrete Slabs-on-Ground," *ACI Materials Journal*, V. 103, No. 1, Jan.-Feb. 2006, pp. 3-10.
19. Buratti, N.; Mazzotti, C.; and Savoia, M., "Post-Cracking Behaviour of Steel and Macro-Synthetic Fibre-Reinforced Concretes," *Construction and Building Materials*, V. 25, No. 5, 2011, pp. 2713-2722.
20. Oh, B. H.; Kim, J. C.; and Choi, Y. C., "Fracture Behavior of Concrete Members Reinforced with Structural Synthetic Fibers," *Engineering Fracture Mechanics*, V. 74, No. 1-2, 2007, pp. 243-257.
21. Otter, D. E., and Naaman, A. E., "Properties of Steel Fiber Reinforced Concrete under Cyclic Loading," *ACI Materials Journal*, V. 85, No. 4, July-Aug. 1988, pp. 254-261.
22. Chalioris, C. E., "Steel Fibrous RC Beams Subjected to Cyclic Deformations under Predominant Shear," *Engineering Structures*, V. 49, 2013, pp. 104-118.
23. Filiatrault, A.; Ladicians, K.; and Massicotte, B., "Seismic Performance of Code-Designed Fiber Reinforced Concrete Joints," *ACI Materials Journal*, V. 91, No. 5, Sept.-Oct. 1994, pp. 564-571.
24. Susetyo, J., "Fibre Reinforcement for Shrinkage Crack Control in Prestressed, Precast Segmental Bridges," PhD dissertation, University of Toronto, Toronto, ON, Canada, 2009, 532 pp.
25. Carnovale, D., "Behaviour and Analysis of Steel and Macro-Synthetic Fibre Reinforced Concrete Subjected to Reversed Cyclic Loading: A Pilot Investigation," MASc dissertation, University of Toronto, Toronto, ON, Canada, 2013, 323 pp.
26. ASTM C1609/C1609M, "Standard Test Methods for Flexural Performance of Fiber-Reinforced Concrete (Using Beam with Third-Point Loading)," ASTM International, West Conshohocken, PA, 2010, 9 pp.

APPENDIX

The following forms an appendix for the journal article entitled “Effect of Fiber Material and Loading History on Shear Behavior of FRC”. Enclosed are supplementary tables and figures supporting the discussion contained in the main body of the article. The results of the cylinder compression tests are given in Table A1, the direct tension results are given in Table A2, the flexural test results in Table A3 and the age of the panel specimens at testing are given in Table A4. A more detailed image of the shear panel test is given in Figure A1, shear panel reinforcement layout is provided in Figure A2, and the failure crack patterns for the panel tests are presented in Figure A3.

Discussion on Direct Tension Tests

Further information worth noting on the direct tension test is given here. The test specimens were loaded in a 55 kips (245 kN) MTS Universal Testing Machine. The specimen was attached to the test machine with a threaded coupler attached to a spherical bearing. Thus, the ends of the specimens were perfectly pinned, meaning that no flexural stresses were transmitted into the specimens. At times in the test program, due to the uneven distribution of fibers within the cracked cross-section, some bending displacements were observed. The at-times uneven distribution of the fibers was a consequence of the small cross-sectional dimensions of the neck of the specimens (75x100 mm or 2.75x4 in) with relatively long fibers (30 to 54 mm or 1.2 to 2.3 in). It made consolidation difficult and occasionally led to uneven distribution of both the fibers and the aggregate, as the fibers tended to form a sieve through which the 10 mm (0.39 in) aggregate could not uniformly distribute. This, in turn, could have potentially affected cracking and crack growth (as the face of a dogbone specimen with more aggregate may crack at a higher load, and the face of the dogbone with more fibers may see a

1 reduced rate of crack growth as the crack is bridged by more fibers). Thus, the results of the
2 dogbone test were treated critically, with due consideration for these effects in the response
3 analysis.

4 Another concern would be restrained shrinkage of the specimens. No reinforcement was
5 placed in the neck of the specimen, to avoid restrained shrinkage of the concrete, and also since
6 the desire was to investigate the pure response in tension of the concrete/fiber composite.

7 **NOTATIONS FOR APPENDIX TABLES:**

8 COV = coefficient of variation

9 E_{cs} = secant modulus of elasticity for concrete in compression

10 E_{ct} = secant modulus of elasticity for concrete in tension

11 f'_c = 28-day compressive strength of concrete

12 f'_t = first cracking strength

13 f_l = flexural first cracking stress

14 f^D_{XXX} = residual flexural stress at midspan displacement of L/XXX

15 f_p = flexural peak stress

16 f_{te} = minimum tensile stress immediately after cracking

17 f_{tu} = ultimate residual tensile stress

18 $R^D_{T,150}$ = equivalent flexural strength ratio

19 T^D_{150} = flexural toughness

20 w_{cr} = crack width

21 $w_{cr,e}$ = crack width at f_{te}

22 $w_{cr,u}$ = crack width at f_{tu}

23 ϵ'_c = strain at peak compressive stress

- 1 ϵ'_t = strain at cracking stress
- 2 ϵ_{c1} = principal tensile strain of concrete
- 3 ϵ_{c2} = principal compressive strain of concrete
- 4

1 TABLES AND FIGURES

2

Table A1–Compression cylinder results

Specimen ID	f'_c , MPa (ksi) [COV]	ϵ'_c , $\times 10^{-3}$ [COV]	E_{cs} , MPa (ksi) [COV]
DC-DB1	58.0 (8.41) [1.19]	2.994 [6.85]	29,900 (4,340) [6.04]
DC-DB2	56.1 (8.14) [0.60]	2.680 [2.25]	34,000 (4,930) [2.99]
DC-P1	71.7 (10.40) [0.55]	2.555 [1.06]	40,200 (5,830) [1.65]
DC-P2	62.1 (9.01) [1.46]	3.169 [5.66]	36,000 (5,220) [3.35]
DC-P3	50.9 (7.38) [1.89]	2.655 [6.25]	32,700 (4,740) [9.45]
DC-P4	64.0 (9.28) [1.23]	3.160 [5.43]	36,000 (5,220) [3.98]
DC-P5	54.3 (7.88) [2.88]	2.877 [4.72]	34,300 (4,975) [5.75]
C1C	65.7 (9.53) [0.30]	2.409 [3.90]	33,500 (4,860) [3.70]
C1F1V1	51.4 (7.45) [1.90]	2.147 [22.8]	32,400 (4,700) [22.7]
C1F1V2	53.4 (7.75)	2.671	32,200 (4,670)

	[5.40]	[15.9]	[26.0]
C1F1V3	49.7 (7.21)	2.504	36,200 (5,250)
	[3.40]	[14.0]	[29.5]

1
2
3
4
5
6
7
8
9
10
11
12
13
14

Table A2–Uniaxial direct tension results

Specimen ID	f'_{ts} MPa (ksi) [COV]	ϵ'_{ts} $\times 10^{-3}$ [COV]	E_{ct} MPa (ksi) [COV]	f_{te} MPa (ksi)	$w_{cr,e}$ mm (in)	f_{tu} MPa (ksi)	$w_{cr,u}$ mm (in)	$f_{cl} @ w_{cr}$ of 3 mm (1/8"), MPa (ksi)
DC-DB1	4.77 (0.692)	0.171 [16.4]	39,400 (5,715)	1.58 (0.229)	0.38 (0.015)	2.36 (0.342)	2.33 (0.092)	2.25 (0.326)

	[7.35]		[12.1]					
DC-DB2	4.80 (0.696) [4.18]	0.140 [15.8]	41,200 (5,975) [5.26]	1.97 (0.286)	0.29 (0.011)	2.95 (0.428)	2.08 (0.082)	2.45 (0.355)
DC-P1	4.35 (0.631) [4.52]	0.148 [9.70]	38,600 (5,600) [9.31]	-	-	-	-	-
DC-P2	3.90 (0.566) [11.5]	0.184 [26.0]	29,000 (4,205) [15.2]	3.20 (0.464)	0.14 (0.006)	3.52 (0.511)	0.65 (0.026)	1.60 (0.232)
DC-P3	4.49 (0.651) [4.59]	0.132 [9.02]	35,700 (5,175) [20.8]	1.58 (0.229)	0.47 (0.019)	1.78 (0.258)	2.51 (0.099)	1.73 (0.251)
DC-P4	4.76 (0.690) [4.33]	0.151 [9.86]	37,900 (5,500) [9.87]	3.49 (0.506)	0.17 (0.007)	3.68 (0.534)	0.27 (0.011)	1.68 (0.244)
DC-P5	4.67 (0.677) [0.24]	0.147 [2.75]	38,100 (5,525) [4.79]	1.61 (0.234)	0.51 (0.020)	2.10 (0.305)	1.59 (0.063)	1.99 (0.289)
C1C	4.07 (0.590) [11.5]	0.101 [12.6]	40,700 (5,900) [12.3]	-	-	-	-	-
C1F1V1	3.75	0.123	30,900	1.67	0.16	1.69	0.19	0.60

	(0.544)	[16.4]	(4,480)	(0.242)	(0.006)	(0.245)	(0.007)	(0.087)
	[13.1]		[1.65]					
C1F1V2	3.46 (0.502) [16.7]	0.127 [20.4]	27,500 (3,990) [11.8]	2.70 (0.392)	0.17 (0.007)	2.87 (0.416)	0.26 (0.010)	1.79 (0.260)
C1F1V3	4.34 (0.629) [7.30]	0.147 [28.4]	32,900 (4,770) [4.5]	3.85 (0.558)	0.17 (0.007)	3.93 (0.570)	0.29 (0.011)	2.32 (0.336)

1
2
3
4
5
6
7
8
9
10
11

Table A3–Flexural test results

Specimen ID	f_l , MPa (ksi) [COV]	f_p , MPa (ksi) [COV]	f^D_{600} , MPa (ksi) [COV]	f^D_{150} , MPa (ksi) [COV]	T^D_{150} , J (ft-lbf) [COV]	$R^D_{T,150}$, % [COV]
DC-P1	7.22	7.22	-	-	-	-

	(1.05)	(1.05)				
	[4.91]	[4.91]				
DC-P3	5.31 (0.77) [13.9]	5.31 (0.77) [13.9]	4.05 (0.59) [10.5]	4.01 (0.58) [15.9]	102.4 (75.5) [14.5]	80.6 [0.00]
DC-P4	6.77 (0.98) [11.5]	8.95 (1.30) [7.11]	8.71 (1.26) [5.69]	5.61 (0.81) [14.5]	179.3 (132.2) [9.85]	110.5 [3.20]
DC-P5	4.88 (0.71) [7.98]	5.45 (0.79) [N/A]	3.41 (0.50) [20.8]	3.89 (0.56) [10.0]	96.3 (71.0) [5.89]	81.9 [0.00]
C1C	3.83 (0.56) [10.1]	3.83 (0.56) [10.1]	-	-	-	-
C1F1V1	7.70 (1.12) [13.4]	7.70 (1.12) [13.4]	4.54 (0.66) [N/A]	2.65 (0.38) [N/A]	92.2 (68.0) [N/A]	51.8 [N/A]
C1F1V2	6.23 (0.90) [9.70]	6.23 (0.90) [9.70]	5.06 (0.73) [N/A]	3.43 (0.50) [N/A]	103.0 (76.0) [N/A]	74.2 [N/A]
C1F1V3	9.26 (1.34) [21.2]	10.29 (1.49) [25.7]	10.08 (1.46) [N/A]	6.55 (0.95) [N/A]	278.2 (205.2) [N/A]	160.7 [N/A]

1
2
3
4
5
6
7
8
9

Table A4—Age of panel specimens at testing

Specimen ID	<i>Age at Testing (Days)</i>
DC-P1	28-31
DC-P2	30
DC-P3	35
DC-P4	42-48
DC-P5	40-41
C1C	N/A
C1F1V1	N/A
C1F1V2	N/A
C1F1V3	N/A

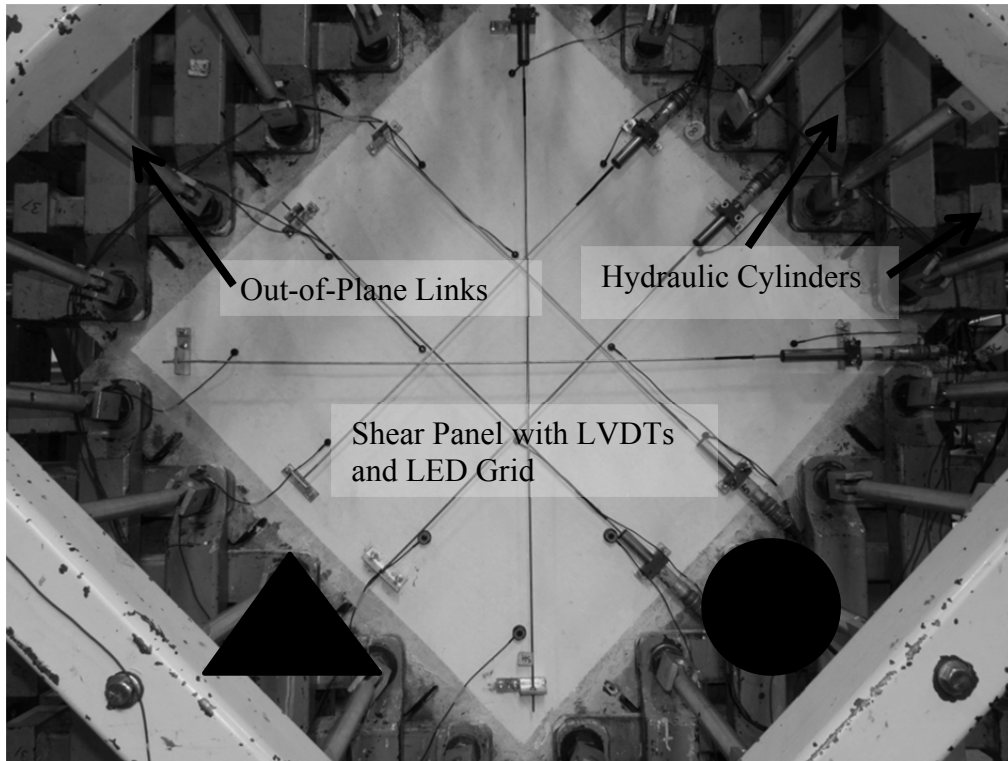
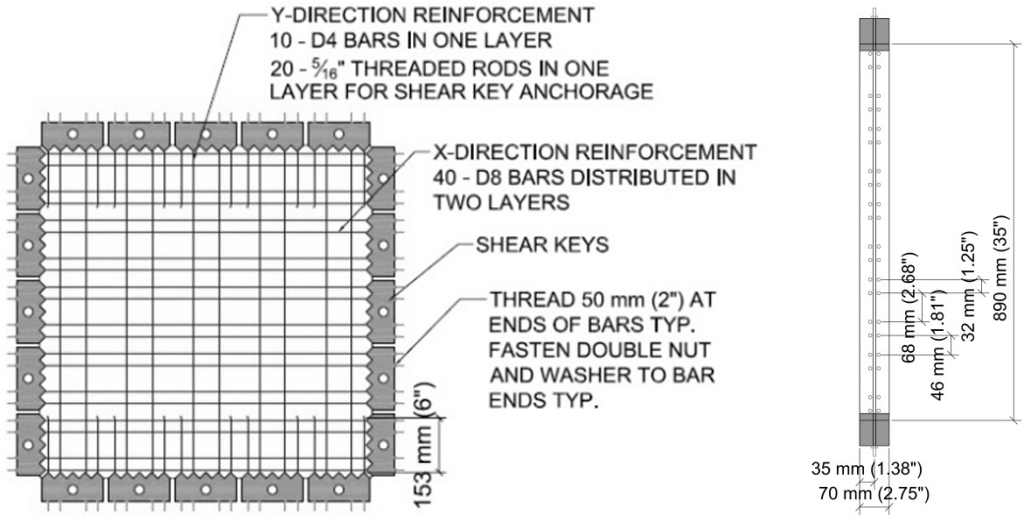
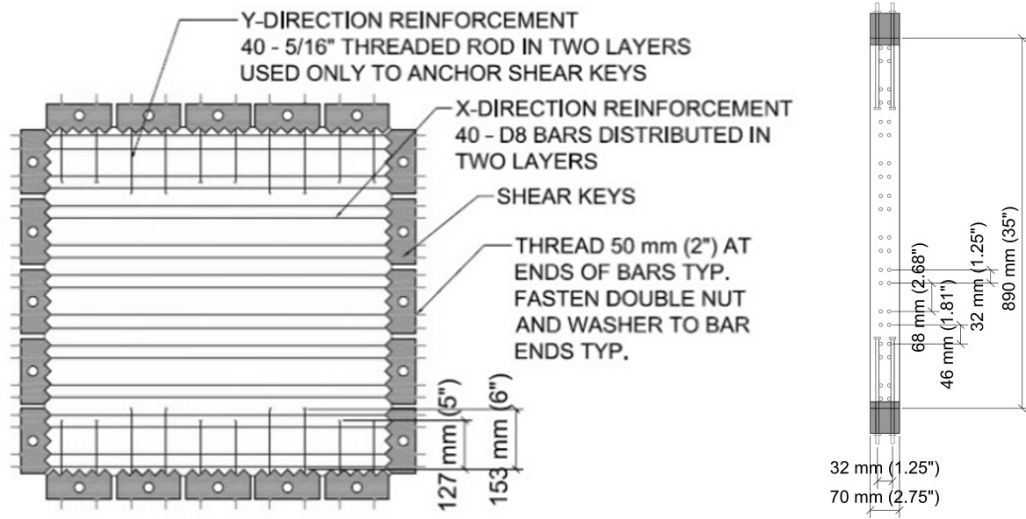


Fig. A1–Panel with Instrumentation, Pin and Roller Location, Out-of-Plane Restraints



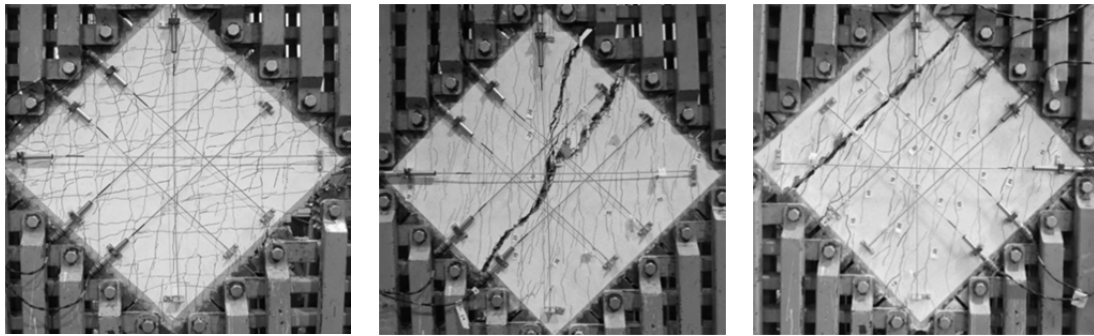
(a)



(b)

- 1
- 2
- 3
- 4
- 5

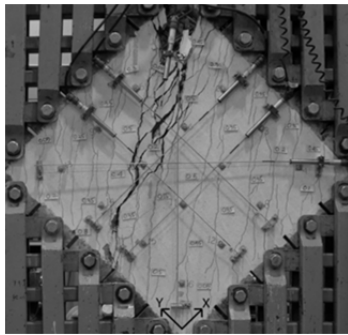
Fig. A2–Shear panel reinforcement layout: (a) plain concrete; (b) FRC.



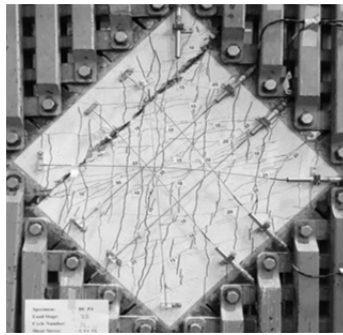
(a)

(b)

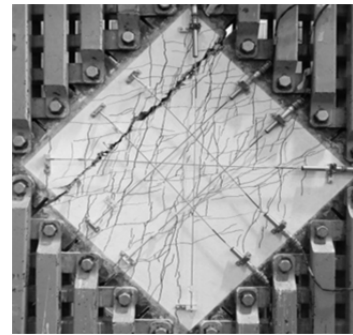
(c)



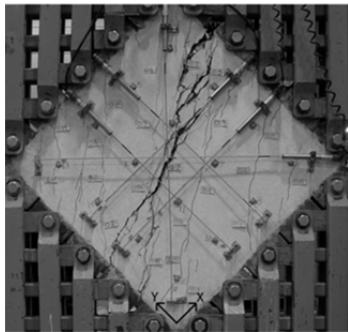
(d)



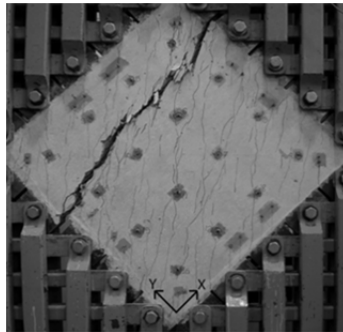
(e)



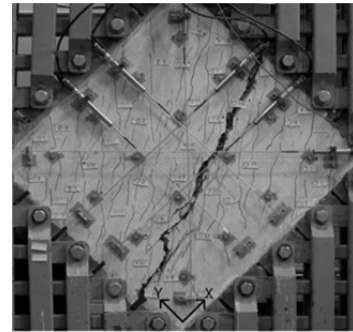
(f)



(g)



(h)



(i)

1 **Fig. A3–Shear panel tests – Failure crack patterns: (a) DC-P1; (b) DC-P2; (c) DC-P3; (d)**

2 **C1C; (e) DC-P4; (f) DC-P5; (g) C1F1V1; (h) C1F1V2; (i) C1F1V3**

3

4

5

6

1
2
3
4
5
6
7
8
9
10
11
12
13
14
15
16
17
18
19
20
21
22
23

List of Tables:

Table A1 – Cylinder compression test results

Table A2 – Uniaxial direct tension test results

Table A3– Flexural (ASTM C1609/C1609M) test results

Table A4– Age of panel specimens at testing

1

2

3

4 **List of Figures:**

5 **Fig. A1** – Panel with Instrumentation, Pin and Roller Location, Out-of-Plane Restraints

6 **Fig. A2** – Shear panel reinforcement layout

7 **Fig. A3** – Failure crack patterns for shear panel tests

8

9